



Cite this: *Phys. Chem. Chem. Phys.*,
2015, 17, 24001

Photoinduced charge accumulation by metal ion-coupled electron transfer[†]

Annabell G. Bonn and Oliver S. Wenger*

An oligotriarylamine (OTA) unit, a Ru(bpy)₃²⁺ photosensitizer moiety (Ru), and an anthraquinone (AQ) entity were combined to a molecular dyad (**Ru-OTA**) and a molecular triad (**AQ-Ru-OTA**). Pulsed laser excitation at 532 nm led to the formation of charge-separated states of the type **Ru⁻-OTA⁺** and **AQ⁻-Ru-OTA⁺** with lifetimes of ≤ 10 ns and 2.4 μ s, respectively, in de-aerated CH₃CN at 25 °C. Upon addition of Sc(OTf)₃, very long-lived photoproducts were observed. Under steady-state irradiation conditions using a flux of $(6.74 \pm 0.21) \times 10^{15}$ photons per second at 450 nm, the formation of twofold oxidized oligotriarylamine (OTA²⁺) was detected in aerated CH₃CN containing 0.02 M Sc³⁺, as demonstrated unambiguously by comparison with UV-Vis absorption spectra obtained in the course of chemical oxidation with Cu²⁺. Photodriven charge accumulation on the OTA unit of **Ru-OTA** and **AQ-Ru-OTA** is possible due to the lowering of the O₂ reduction potential caused by the interaction of superoxide with the strong Lewis acid Sc³⁺. The presence of the anthraquinone unit in **AQ-Ru-OTA** accelerates the rate-determining reaction step for charge accumulation by a factor of 10 compared to the **Ru-OTA** dyad. This is attributed to the formation of Sc³⁺-stabilized anthraquinone radical anion intermediates in the triad. Possible mechanistic pathways leading to charge accumulation are discussed. Photodriven charge accumulation is of key importance for solar fuels because their production will have to rely on multi-electron chemistry rather than single-electron reaction steps. Our study is the first to demonstrate that metal ion-coupled electron transfer (MCET) can be exploited to accumulate charges on a given molecular unit using visible light as an energy input. The approach of using a combination of intra- and intermolecular electron transfer reactions which are enabled by MCET is conceptually novel, and the fundamental insights gained from our study are relevant in the greater context of solar energy conversion.

Received 8th August 2015,
Accepted 11th August 2015

DOI: 10.1039/c5cp04718h

www.rsc.org/pccp

1. Introduction

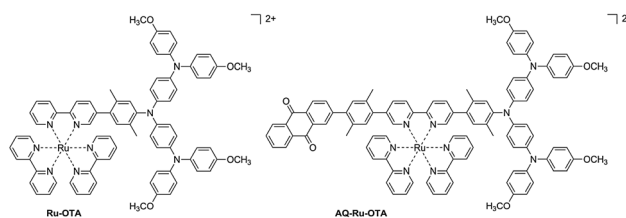
The primary events of natural photosynthesis are light absorption, energy transfer, and electron transfer.¹ In the course of the Kok cycle, oxidative equivalents are accumulated on a calcium-containing manganese cluster, the so-called oxygen-evolving complex (OEC).² In recent years, considerable efforts have been devoted to the development of artificial OECs, and in many cases it has been possible to catalyze the oxidation of water with sacrificial reagents such as Ce(IV) salts.³ The generation of solar fuels (e.g., H₂ from H₂O; methanol or methane from CO₂) will inevitably require multi-electron chemistry, and in this greater context it is desirable to gain a more thorough understanding of how charges can be accumulated on a given molecular unit,⁴ ideally using visible light as an energy source.⁵

Department of Chemistry, University of Basel, St. Johanns-Ring 19, 4056 Basel, Switzerland. E-mail: oliver.wenger@unibas.ch

† Electronic supplementary information (ESI) available: Synthetic protocols, product characterization data, and additional optical spectroscopic and electrochemical data. See DOI: 10.1039/c5cp04718h

Photoinduced charge accumulation has received significant attention in recent years.^{5b,6} Recent studies demonstrated that 10 or more charges can readily be accumulated in nanoparticles,⁷ but in purely molecular systems already the accumulation of 2 electrons or holes represents a significant challenge.⁸ While systems based on nanoparticles are promising for applications, control over sample heterogeneity (e.g., regarding particle size and binding equilibria of redox-active surfactants) can be tricky to obtain, and one is often confronted with complications resulting from the involvement of surface states.⁹ For fundamental and mechanistic investigations, purely molecular systems therefore remain attractive. In the vast majority of cases explored to date, sacrificial redox reagents were used (e.g., triethylamine for reduction and peroxydisulfate for oxidation processes),¹⁰ and there are only very few exceptions.^{6g,8a,b,11} Using sacrificial reagents, photoinduced charge accumulation in purely molecular systems has been achieved for example in quinone-based triads,^{6d-f} in various coordination compounds containing precious metals such as Rh, Ir, Pd or Pt,^{6b,c,12} and in many cobaloximes in which the accumulation of two negative charges was employed for the formation of H₂.¹³ Many other examples from the realms of





Scheme 1 Chemical structures of the **Ru-OTA** dyad and the **AQ-Ru-OTA** triad investigated in this work.

biomimetic chemistry could be mentioned in this context.¹⁴ In several cases of hydrogen-evolving complexes it is not *a priori* clear whether charge accumulation indeed occurs on a molecular catalyst, or whether a colloid formed in the course of photo-irradiation is the catalytically active species.¹⁵ This important issue has been intensely debated in the recent past, and against this background it seems all the more relevant to explore chemically well-defined systems in which photoinduced charge accumulation can be detected unambiguously. The majority of prior studies of photo-production of H₂, photo-oxidation of H₂O, or photo-reduction of CO₂ have not focused on the elementary steps of charge accumulation.

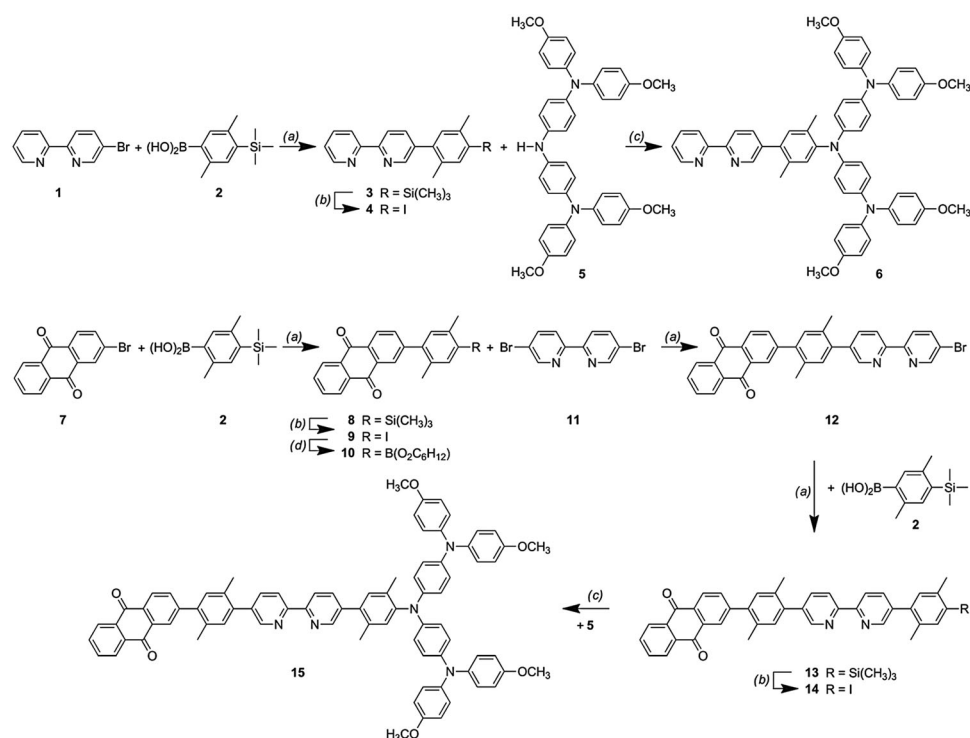
We report here on the use of metal ion-coupled electron transfer (MCET) for photoinduced accumulation of two positive charges on the oligotriarylamine (OTA) units of the two compounds from Scheme 1. The first compound (**Ru-OTA**) is a molecular dyad comprised of an OTA donor unit which is connected to a Ru(bpy)₃²⁺ (bpy = 2,2'-bipyridine) photosensitizer.

The second compound (**AQ-Ru-OTA**) is a molecular triad which contains an additional 9,10-anthraquinone (AQ) acceptor unit. Photoexcitation of the Ru(bpy)₃²⁺ complex of **Ru-OTA** and **AQ-Ru-OTA** in the presence of oxygen and the strong Lewis acid Sc³⁺ leads to the formation of OTA²⁺ in both compounds, because MCET greatly stabilizes the superoxide reduction product. The stabilization of O₂⁻ and quinone radical anions by various Lewis acids has been investigated in considerable detail, and the term MCET has been coined by Fukuzumi.¹⁶ Others have demonstrated how the Lewis acidity of a redox-inactive metal in artificial manganese clusters mimicking the naturally occurring OEC affects the redox properties, thereby illustrating the possible role of Ca²⁺ in the biological Mn₄ cluster.¹⁷ We are unaware of prior studies in which Lewis acids have been employed to achieve visible light-driven accumulation of positive charge carriers on a molecular unit.

2. Results and discussion

Synthesis

The key ligand of the **Ru-OTA** dyad was prepared as illustrated in the uppermost line of Scheme 2. 5-Bromo-2,2'-bipyridine (**1**)¹⁸ was reacted with (2,5-dimethyl-4-(trimethylsilyl)phenyl)boronic acid (**2**)¹⁹ under standard Suzuki cross-coupling conditions, and the trimethylsilyl protection group of the coupling product (**3**) was substituted by an iodine atom using ICl.¹⁹ The resulting iodo-compound (**4**) was reacted with oligotriarylamine 5^{8b,20} in a Pd(0) catalyzed N-C coupling reaction to afford ligand **6**,



Scheme 2 Synthesis of the key ligands of the **Ru-OTA** dyad and the **AQ-Ru-OTA** triad: (a) Na₂CO₃, Pd(PPh₃)₄, toluene, ethanol, and H₂O; (b) ICl and CH₂Cl₂/CH₃CN; (c) NaO^tBu, Pd(dba)₂, (HP^tBu₃)BF₄, and toluene; (d) bis(pinacolato)diborane, KOAc, PdCl₂(PPh₃)₂, and DMF.



which was subsequently refluxed together with $\text{Ru}(\text{bpy})_2\text{Cl}_2$ to yield the **Ru-OTA** dyad. The overall yield for the synthesis of **Ru-OTA** was 61% with respect to 5-bromo-2,2'-bipyridine (**1**).

The key ligand of the **AQ-Ru-OTA** triad was synthesized as shown in the middle and lower part of Scheme 2. After cross-coupling of 2-bromo-9,10-anthraquinone (**7**) and (2,5-dimethyl-4-(trimethylsilyl)phenyl)boronic acid (**2**),¹⁹ the trimethylsilyl group of the reaction product (**8**) was substituted by an iodine atom using ICl to afford iodo-compound **9**. In a Pd-catalyzed reaction with bis(pinacolato)diborane, the iodine atom of compound **9** was then replaced by a boronic ester group to afford compound **10**. The latter was reacted with one equivalent of 5,5'-dibromo-2,2'-bipyridine (**11**) under standard Suzuki coupling conditions to yield compound **12**. Subsequent reaction with (2,5-dimethyl-4-(trimethylsilyl)phenyl)boronic acid (**2**)¹⁹ gave compound **13**, and the trimethylsilyl group of the latter was replaced by an iodine atom using ICl. The resulting iodo-compound **14** was reacted with oligotriarylamine **5**^{8b,20} in a Pd-catalyzed N-C coupling reaction to afford ligand **15**, which was subsequently coordinated to $\text{Ru}(\text{bpy})_2\text{Cl}_2$ to give the **AQ-Ru-OTA** triad. The overall yield for the synthesis of **AQ-Ru-OTA** was 14% with respect to the 2-bromo-9,10-anthraquinone (**7**) starting material. Complete synthesis procedures and product characterization data are given in the ESI.[†]

Electrochemistry

Cyclic voltammetry was performed in dry, de-aerated CH_3CN using 0.1 M TBAPF₆ (tetra-*n*-butylammonium hexafluorophosphate) as a supporting electrolyte. The main purpose of these investigations was to establish the thermodynamics of photoinduced charge accumulation on the oligotriarylamine units of **Ru-OTA** and **AQ-Ru-OTA**. Voltammograms measured at a potential sweep

Table 1 Electrochemical potentials (E^0 in Volts vs. Fc^+/Fc) of the individual redox-active units of **Ru-OTA**, **AQ-Ru-OTA**, and the $\text{Ru}(\text{bpy})_3^{2+}$ reference complex in CH_3CN ^a

	Ru-OTA	AQ-Ru-OTA	$\text{Ru}(\text{bpy})_3^{2+}$
$\text{Ru}^{(\text{III/II})}$	0.94	0.91	0.90
$\text{bpy}^{0/-}$	-1.68	-1.66	-1.72
$\text{bpy}^{0/-}$	-1.88		-1.92
$\text{bpy}^{0/-}$	-2.11		-2.17
$\text{OTA}^{+/0}$	-0.02	-0.06	
$\text{OTA}^{2+/+}$	0.24	0.20	
$\text{OTA}^{3+/2+}$	0.68	0.64	
$\text{AQ}^{0/-}$		-1.26	

^a Data extracted from the cyclic voltammograms shown in Fig. 1.

rate of 0.1 V s^{-1} are shown in Fig. 1 for (a) **Ru-OTA**, (b) **AQ-Ru-OTA**, and (c) the $\text{Ru}(\text{bpy})_3^{2+}$ reference complex. The electrochemical potentials extracted from these data are summarized in Table 1. Comparison of Fig. 1a and b with Fig. 1c readily permits the identification of redox waves which are either caused by the oxidation of $\text{Ru}(\text{II})$ to $\text{Ru}(\text{III})$, or by the consecutive one-electron reduction of the three bpy ligands. No significant differences in the respective redox potentials are observed between **Ru-OTA**/**AQ-Ru-OTA** and the reference complex, *i.e.*, the electrochemical behavior of the ruthenium complex in the dyad and the triad is essentially unperturbed by the OTA-functionalized ligand.

Three quasi-reversible one-electron oxidation waves are detected for the oligotriarylamine unit of **Ru-OTA** and **AQ-Ru-OTA**, as commonly observed.^{8b,20,21} The first two oxidations occur at around 0.0 and 0.2 V vs. Fc^+/Fc with separations between cathodic and anodic peak currents ($E_{\text{p,c}} - E_{\text{p,a}}$) of approximately 80 mV, while the third oxidation occurs at around 0.6 V vs. Fc^+/Fc with $(E_{\text{p,c}} - E_{\text{p,a}}) \approx 170 \text{ mV}$. The first two oxidations of oligotriarylamines are usually more reversible than higher oxidations.^{8b,20,21}

Reduction of the anthraquinone unit of **AQ-Ru-OTA** is detected at -1.26 V vs. Fc^+/Fc , in line with expectation based on previously investigated related compounds.^{20,22} All electrochemical potentials in Table 1 are in good agreement with previously reported values for $\text{Ru}(\text{bpy})_3^{2+}$,²³ oligotriarylamines,^{8b,21} and anthraquinones.²²

Optical absorption and luminescence spectroscopy

The UV-Vis absorption spectra of **Ru-OTA**, **AQ-Ru-OTA**, and $\text{Ru}(\text{bpy})_3^{2+}$ in CH_3CN are shown in Fig. 2. In addition to the

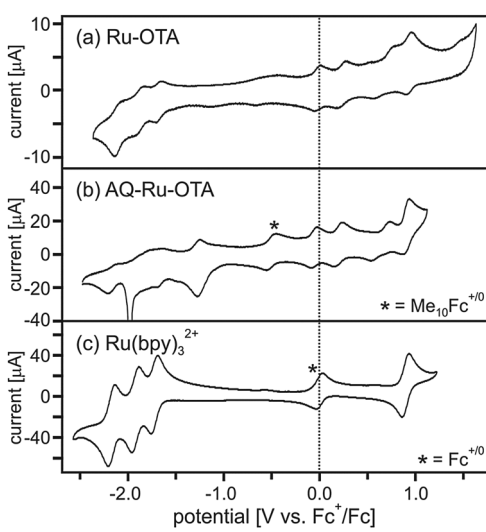


Fig. 1 Cyclic voltammograms of (a) **Ru-OTA**, (b) **AQ-Ru-OTA**, and (c) $\text{Ru}(\text{bpy})_3^{2+}$ in dry, de-aerated CH_3CN with 0.1 M TBAPF₆ obtained at a potential sweep rate of 0.1 V s^{-1} . The asterisks (*) mark waves due to ferrocene (c) or decamethylferrocene (b) which was added in small quantities for internal potential calibration. The strongly negative current around -2.0 V vs. Fc^+/Fc in (b) is attributed to an adsorption process.

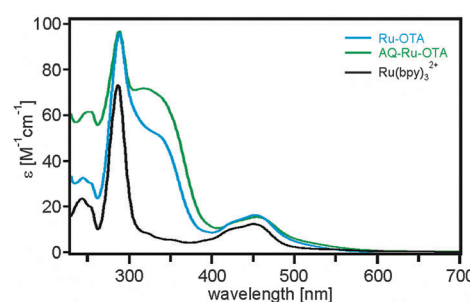


Fig. 2 UV-Vis absorption spectra of the two compounds from Scheme 1 and the $\text{Ru}(\text{bpy})_3^{2+}$ reference complex in CH_3CN at 25°C .

$^1\text{MLCT}$ absorption band at ~ 450 nm and a bpy-centered $\pi-\pi^*$ absorption at around 290 nm, the dyad and the triad exhibit absorption at around 330 nm, which can be attributed to the oligotriarylamine and anthraquinone units.

The oligotriarylamine unit of **Ru-OTA** and **AQ-Ru-OTA** can readily be oxidized to its mono- and dicationic forms with $\text{Cu}(\text{ClO}_4)_2$ because the reduction potential of the latter is 0.57 V vs. Fc^+/Fc in CH_3CN .²⁴ For the series of UV-Vis difference spectra in Fig. 3a, the absorption spectrum of 10^{-5} M **Ru-OTA** in CH_3CN was used as a baseline, and the individual spectra were recorded after the addition of increasing amounts of $\text{Cu}(\text{ClO}_4)_2$. The green trace was obtained after adding 1 equivalent of chemical oxidant. In the respective spectrum, absorption bands at 430, 735, and 1310 nm are prominent, and they are attributed to OTA^+ , in line with prior studies.^{8b,20} Upon addition of a second equivalent of $\text{Cu}(\text{ClO}_4)_2$, the abovementioned bands disappear, and new bands at 595 and 1130 nm gain intensity, compatible with the formation of OTA^{2+} (red trace).^{8b,20} Analogous experiments with **AQ-Ru-OTA** (Fig. 3b) provide very similar results. The key finding from these chemical oxidation experiments is that one- and two-electron oxidation products (OTA^+ vs. OTA^{2+}) can easily be distinguished from each other on the basis of UV-Vis spectroscopy.

In passing we note that based on the abovementioned redox potentials, the oxidation of OTA to OTA^{2+} by $\text{Cu}(\text{n})$ is essentially complete. For instance, the equilibrium constant for the reaction $\text{Ru-OTA}^+ + \text{Cu}(\text{n}) \rightleftharpoons \text{Ru-OTA}^{2+} + \text{Cu}(\text{i})$ is 3.8×10^5 . Only marginal amounts of $\text{Cu}(\text{n})$ therefore remain in solution, and these cannot account for the absorption features in Fig. 3.

Photoexcitation of de-aerated CH_3CN solutions at 450 nm shows that the emission of **Ru-OTA** and **AQ-Ru-OTA** is much

weaker than that of $\text{Ru}(\text{bpy})_3^{2+}$ under identical conditions, indicating that the lowest $^3\text{MLCT}$ excited state of the dyad and the triad is depopulated efficiently by a nonradiative process (data not shown). After pulsed excitation of de-aerated CH_3CN solutions at 532 nm, the luminescence lifetimes are 830 ns for $\text{Ru}(\text{bpy})_3^{2+}$, ≤ 10 ns for **Ru-OTA**, and ≤ 10 ns for **AQ-Ru-OTA** (data not shown). The luminescence lifetimes of the dyad and the triad are instrumentally limited, and this finding is compatible with their weak luminescence intensities relative to $\text{Ru}(\text{bpy})_3^{2+}$.

Nanosecond transient absorption

Following excitation of $(2.5 \pm 0.2) \times 10^{-5}$ M solutions of **Ru-OTA** and **AQ-Ru-OTA** in de-aerated CH_3CN at 532 nm with laser pulses of ~ 10 ns duration, the transient difference spectra shown in Fig. 4a and b are obtained. Acquisition of these spectra occurred by time-averaging over a period of 200 ns immediately after laser excitation. Both spectra exhibit a bleach at ~ 335 nm, an intense positive band at ~ 415 nm, and a weaker band beginning at ~ 635 nm and extending to ~ 800 nm. The spectrum of the triad exhibits an additional band at ~ 565 nm, and in the spectrum of the dyad a relatively weak additional band at ~ 520 nm can be seen.

The UV-Vis difference spectra shown in Fig. 4c and d are the green traces from Fig. 3a and b, *i.e.* these are the difference spectra between Ru-OTA^+ (or AQ-Ru-OTA^+) and **Ru-OTA** (or **AQ-Ru-OTA**). The agreement between transient absorption (Fig. 4a and b) and UV-Vis difference spectra obtained from chemical oxidation experiments (Fig. 4c and d) is remarkable, and one can immediately conclude that the OTA^+ oxidation product is formed in the transient absorption experiments. The reduction product can readily be identified as a reduced ruthenium photosensitizer in the case of the dyad (transient absorption band at ~ 520 nm in Fig. 4a),²⁵ and as reduced anthraquinone in the case of the triad (transient absorption band at ~ 565 nm in Fig. 4b).²⁶ Thus, there is clear evidence for intramolecular photoinduced electron transfer after pulsed excitation of the two compounds from Scheme 1, resulting in the formation of $\text{Ru}^-\text{-OTA}^+$ and $\text{AQ}^-\text{-Ru-OTA}^+$ photoproducts. The reaction free energy for electron

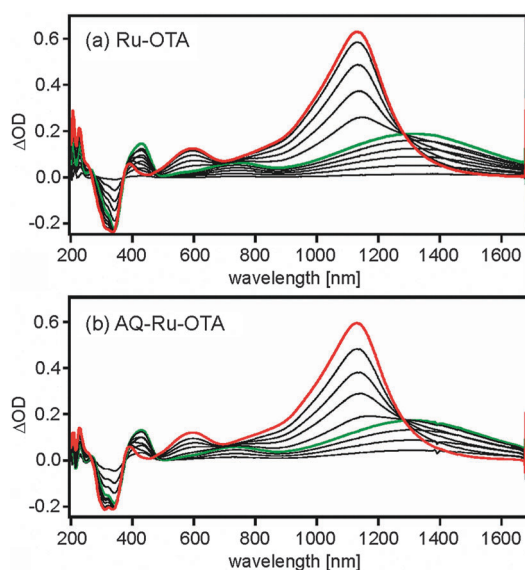


Fig. 3 UV-Vis difference spectra measured in the course of chemical oxidation of the dyad and the triad with $\text{Cu}(\text{ClO}_4)_2$ in aerated CH_3CN at 25 °C. The spectra of **Ru-OTA** (a) and **AQ-Ru-OTA** (b) measured prior to the addition of any oxidant served as baselines. The individual shown spectra were measured after adding increasing amounts of $\text{Cu}(\text{ClO}_4)_2$. The green traces are attributed to $\text{Ru-OTA}^+/\text{AQ-Ru-OTA}^+$, and the red traces are assigned to $\text{Ru-OTA}^{2+}/\text{AQ-Ru-OTA}^{2+}$.

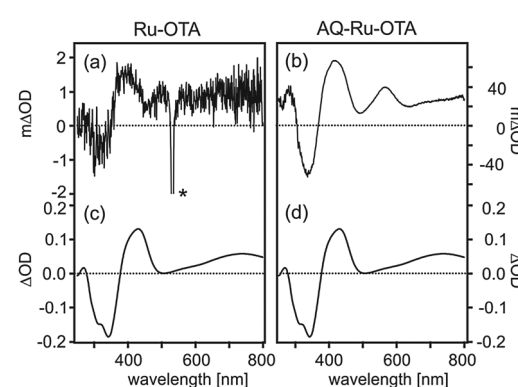


Fig. 4 Transient absorption spectra measured after excitation of (a) **Ru-OTA** and (b) **AQ-Ru-OTA** in de-aerated CH_3CN at 25 °C with laser pulses of ~ 10 ns duration at 532 nm. The spectra were acquired by time-integration over the first 200 ns following excitation. The asterisk (*) marks a signal due to laser stray light. The spectra in (c) and (d) are the green traces from Fig. 3a and b, *i.e.* the UV-Vis difference spectra obtained for Ru-OTA^+ and $\text{AQ}^-\text{-Ru-OTA}^+$.



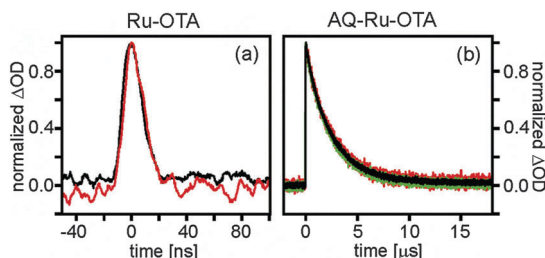


Fig. 5 Temporal evolution of the transient absorption signals observed in Fig. 4 for the dyad at 400 nm (black trace in panel a) and 650 nm (red trace in panel a), and for the triad at 415 nm (black trace in panel b), at 685 nm (red trace in panel b), and at 565 nm (green trace in panel b).

transfer from OTA to the 3 MLCT-excited photosensitizer is approximately -0.5 eV (see ESI,[†] for details).

As seen from Fig. 5a and b, the **Ru⁺-OTA⁺** and **AQ⁻-Ru-OTA⁺** photoproducts are formed within the ~ 10 ns duration of the excitation laser pulses. Our own recent work on closely related triarylamine-Ru(bpy)₃²⁺ and triarylamine-Ru(bpy)₃²⁺-anthraquinone compounds (using equipment with higher temporal resolution) strongly suggests that the **Ru⁺-OTA⁺** and **AQ⁻-Ru-OTA⁺** charge-separated states are actually formed with rate constants on the order of 10^{10} – 10^{11} s⁻¹.^{22,27}

In de-aerated CH₃CN, the transient absorption signal of the dyad at 400 nm decays with an instrumentally limited lifetime of ~ 10 ns (black trace in Fig. 5a), explaining the low signal-to-noise ratio in the transient difference spectrum of Fig. 4a. In the triad, the transient absorption signals at 415, 565, and 685 nm all decay with a lifetime of 2.4 μ s (Fig. 5b), indicating that the OTA⁺ and AQ⁻ photoproducts disappear in a single reaction step involving thermal electron transfer from the reduced anthraquinone to the oxidized oligotriarylamine, as commonly observed in such triads.^{22,26a,c,27,28}

Importantly, no evidence could be obtained for photoinduced charge accumulation on either OTA or AQ in de-aerated CH₃CN using pulsed laser excitation. Since prior studies demonstrated that Lewis acids can stabilize quinone radical anions,¹⁶ we wondered whether the addition of Sc³⁺ could enable photoinduced charge accumulation in **AQ-Ru-OTA**. However, when adding 2000 equivalents of Sc(OTf)₃ to 10^{-5} M solutions of **Ru-OTA** and **AQ-Ru-OTA** in CH₃CN, the samples did undergo rapid color changes upon exposure to light. Nanosecond transient absorption studies were essentially impossible to perform in the presence of Sc³⁺, because a stable photoproduct accumulated between laser flashes. Even single-shot experiments were essentially impossible to perform because some OTA⁺ photoproducts were formed already during sample preparation due to unavoidable light exposure. Moreover, in the transient absorption experiments the probe beam alone induced significant photoreaction. We therefore turned to experiments in which the compounds from Scheme 1 were irradiated continuously with visible light.

Continuous photo-irradiation in the presence of Sc³⁺

For these experiments, $(1.0 \pm 0.1) \times 10^{-5}$ M solutions of the **Ru-OTA** dyad and the **AQ-Ru-OTA** triad in 3 ml of CH₃CN containing 0.02 M of Sc(OTf)₃ were irradiated in a thermostated

cell compartment of a fluorimeter. The latter provided a flux of $(6.74 \pm 0.21) \times 10^{15}$ photons per second at 450 nm, as determined by ferrioxalate actinometry.²⁹ The irradiated area was approximately 0.5 cm². The series of UV-Vis difference spectra in Fig. 6 were recorded after different irradiation times; in general the baseline is the UV-Vis spectrum of the dyad (left) or the triad (right) measured immediately after sample preparation. The red traces were all recorded after one hour of irradiation with the abovementioned photon flux, *i.e.* with a total number of $(2.43 \pm 0.08) \times 10^{19}$ photons (corresponding to $(4.0 \pm 0.1) \times 10^{-5}$ mol of photons).

In Fig. 6a the UV-Vis difference spectra measured for 10^{-5} M **Ru-OTA** in aerated CH₃CN with 0.02 M Sc(OTf)₃ are shown. Comparison with the UV-Vis difference spectra obtained after oxidation with Cu(ClO₄)₂ (Fig. 3a) shows that **Ru-OTA⁺** (with its characteristic band at 1320 nm) is formed over the first 4 minutes (green trace) of photo-irradiation, but after 1 hour (red trace) **Ru-OTA²⁺** (with its diagnostic band at 1130 nm) is clearly the dominant species. (The data are shown in more detail in Fig. S2 (ESI[†]), which clearly demonstrates that no reduced ruthenium is present.)

Fig. 6e shows analogous UV-Vis difference spectra of 10^{-5} M **AQ-Ru-OTA** in aerated CH₃CN with 0.02 M Sc(OTf)₃. In this case, already after 1 minute of irradiation time (green trace) a substantial amount of **AQ-Ru-OTA⁺** is present. After 1 hour (red trace), **AQ-Ru-OTA²⁺** is clearly the dominant species. In fact, already the solution used for recording the baseline spectrum at $t = 0$ contains a significant amount of **AQ-Ru-OTA⁺**, and this causes the bleach (negative signal) in the absorption spectra at around 1300 nm with increasing irradiation time (see ESI,[†] for details). (The data are shown in more detail in Fig. S3 (ESI[†]), which clearly demonstrates that no reduced ruthenium or reduced anthraquinone is present.)

A series of reference experiments were performed to elucidate under what conditions OTA²⁺ formation in **Ru-OTA** and **AQ-Ru-OTA** can occur. In the dark, OTA²⁺ is not formed, neither in the dyad (Fig. 6b) nor in the triad (Fig. 6f). In the respective UV-Vis difference spectra one merely recognizes a weak band centered at around 1320 nm which is attributed to thermal oxidation of OTA by O₂. We recall that the red traces were recorded after 1 hour.

When freeze-pump-thaw de-oxygenated 10^{-5} M CH₃CN solutions of **Ru-OTA** and **AQ-Ru-OTA** with 0.02 M Sc³⁺ are photo-irradiated, OTA²⁺ is not formed (Fig. 6c and g). Instead, only weak absorption bands centered at 1320 nm are detected, indicating the formation of small amounts of OTA⁺. This is attributed to oligotriarylamine oxidation caused by trace amounts of O₂ which remain in solution after the freeze-pump-thaw process. We estimate that the amount of residual O₂ in our cuvettes is on the order of 5×10^{-9} mol, and the amounts of **Ru-OTA⁺** and **AQ-Ru-OTA⁺** formed as shown in Fig. 6c and g are similar.

Irradiation of 10^{-5} M **Ru-OTA** and **AQ-Ru-OTA** solutions in aerated CH₃CN in the absence of Sc³⁺ does not lead to any observable photoproducts at all (Fig. 6d and h). After 1 hour of irradiation, one still obtains basically the baseline spectrum.

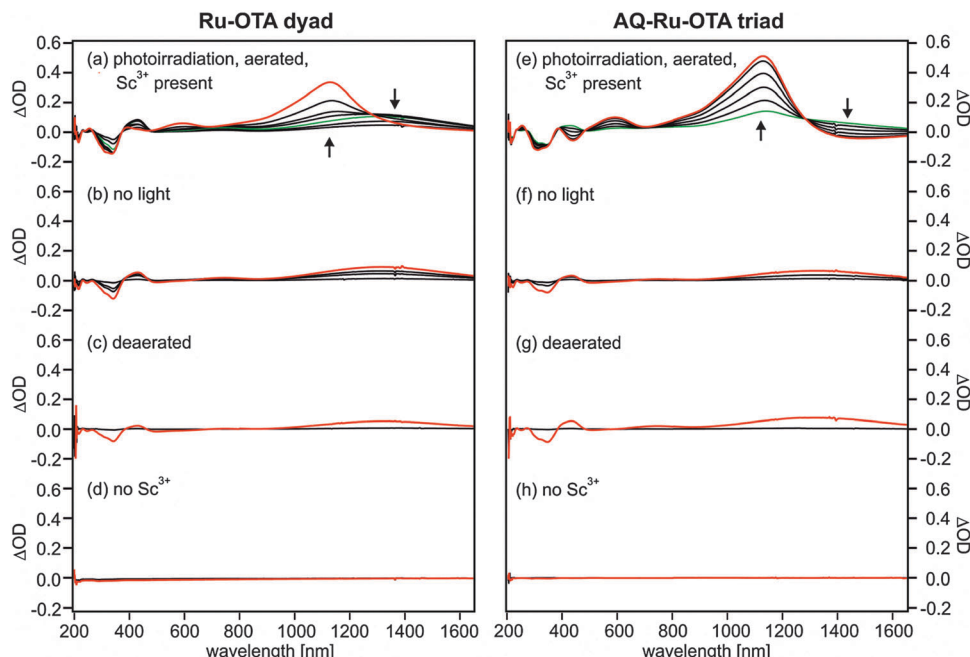


Fig. 6 UV-Vis difference spectra measured on 10^{-5} M solutions of the dyad (left) and the triad (right) in CH_3CN under various conditions (see insets). The UV-Vis spectra of **Ru-OTA/AQ-Ru-OTA** recorded immediately after sample preparation served as baselines in all cases. Individual traces were recorded after different time intervals; the red traces were measured after 60 minutes in all cases. Where applicable, samples were irradiated with a flux of $(6.74 \pm 0.21) \times 10^{15}$ photons per second at 450 nm. Conditions were as follows: (a and e) samples were photoirradiated in aerated CH_3CN in the presence of 0.02 M $\text{Sc}(\text{OTf})_3$; (b and f) aerated CH_3CN samples were left in the dark in the presence of 0.02 M $\text{Sc}(\text{OTf})_3$; (c and g) samples containing 0.02 M $\text{Sc}(\text{OTf})_3$ were de-aerated using a freeze-pump-thaw technique prior to photoirradiation; (d and h) aerated samples without any Sc^{3+} were photoirradiated.

The combination of experiments summarized in Fig. 6 clearly demonstrates that charge-accumulation on the oligotriarylamine units of **Ru-OTA** and **AQ-Ru-OTA** is a photoinduced process which requires O_2 and Sc^{3+} to be simultaneously present. When either light, O_2 , or Sc^{3+} is missing, OTA^{2+} is not formed. Prior studies demonstrated that strong Lewis acid/Lewis base interaction between Sc^{3+} and superoxide anions has important thermodynamic consequences for oxygen reduction.^{16a,b,e} In pure CH_3CN the reduction potential of O_2 is -1.25 V vs. Fc^+/Fc ,³⁰ but in the presence of $\text{Sc}(\text{hmpa})_3^{3+}$ a reduction potential of -0.2 V vs. Fc^+/Fc has been reported for O_2 in propionitrile.^{16e} Consequently, there is a substantial driving-force for photoinduced O_2 reduction in the presence of Sc^{3+} , and this makes charge accumulation on the oligotriarylamine units of **Ru-OTA** and **AQ-Ru-OTA** possible.

Mechanisms for charge accumulation

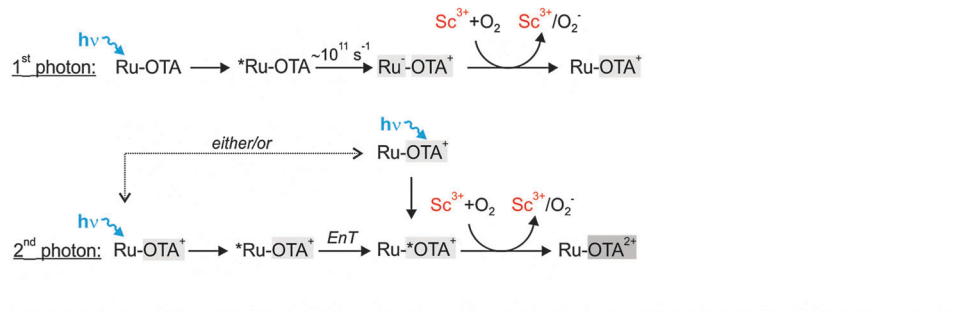
Intramolecular photoinduced electron transfer to establish the **Ru⁻-OTA⁺** and **AQ⁻-Ru-OTA⁺** charge separated states (Fig. 4) takes place with rate constants on the order of 10^{10} – 10^{11} s⁻¹ (Scheme 3a and b, uppermost lines), as discussed above.^{22,27} Subsequent bimolecular electron transfer with O_2 in the presence of Sc^{3+} can then occur with essentially diffusion-limited kinetics, because of the high driving force for the formation of $\text{Sc}^{3+}/\text{O}_2^-$ adducts (see above). Given an O_2 solubility of 8 mM in CH_3CN at room temperature³¹ and a diffusion constant of 1.9×10^{10} M⁻¹ s⁻¹ for O_2 in CH_3CN at 298 K,³² we estimate that O_2 reduction occurs with a pseudo-first order rate constant of

1.5×10^8 s⁻¹. This is competitive with decay of the **Ru⁻-OTA⁺** photoproduct by intramolecular thermal electron transfer, which has been found above to occur with a rate constant of $\geq 10^8$ s⁻¹ (Fig. 5a). However, the **AQ⁻-Ru-OTA⁺** state of the triad decays only with a rate constant of 3.8×10^5 s⁻¹ (Fig. 5b), and consequently bimolecular electron transfer with O_2 should be far more efficient in this case. The time evolution and quantum yield studies discussed below provide indirect support for this assessment. Moreover, benzoquinone reductions in CH_3CN typically become easier by *ca.* 1.1 V due to strong Lewis acid/Lewis base interaction between Sc^{3+} and benzoquinone radical anions.¹⁶ Consequently, the **AQ⁻-Ru-OTA⁺** photoproduct is further stabilized in the presence of Sc^{3+} ($\text{Sc}^{3+}/\text{AQ}^-\text{-Ru-OTA}^+$ state on the first line of Scheme 3b), and this increases the probability for collisional encounters with O_2 that lead to the formation of $\text{Sc}^{3+}/\text{O}_2^-$ adducts *via* bimolecular electron transfer. Thus, after the absorption of a first photon, the photoproducts are **Ru-OTA⁺** or **AQ-Ru-OTA⁺** and one equivalent of $\text{Sc}^{3+}/\text{O}_2^-$ adduct (Scheme 3a and b, uppermost lines). The beneficial effect of Sc^{3+} originates mostly in the fact that it stabilizes O_2^- against recombination with the oxidation products, thereby permitting charge accumulation. The mechanistic question whether MCET takes place in a concerted or stepwise fashion is beyond the scope of this study.

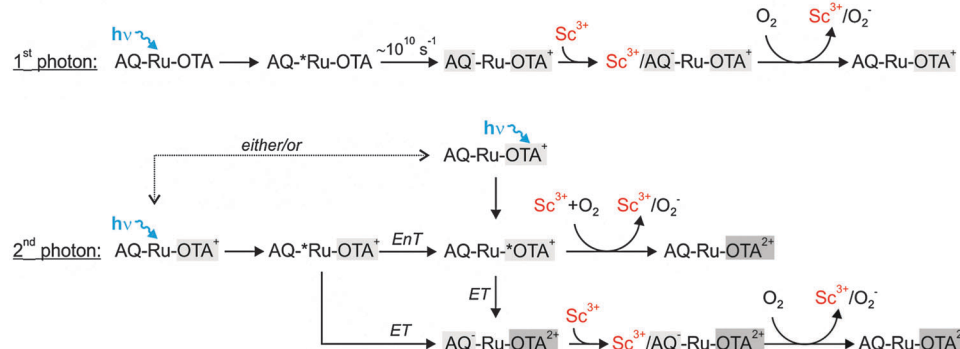
Subsequent absorption of a second photon can occur either by the $\text{Ru}(\text{bpy})_3^{2+}$ photosensitizer or the OTA^+ units of **Ru-OTA⁺** or **AQ-Ru-OTA⁺**. At the irradiation wavelength of 450 nm, the relevant extinction coefficients are 1.3×10^4 M⁻¹ cm⁻¹



(a) dyad



(b) triad



Scheme 3 Possible mechanistic pathways leading to the accumulation of positive charges on the oligotriarylamine unit of (a) **Ru-OTA** and (b) **AQ-Ru-OTA** following the consecutive absorption of two photons. (Energy-wasting reaction pathways which do not lead to charge accumulation are not included for the sake of simplicity).

($\text{Ru}(\text{bpy})_3^{2+}$) and $10^4 \text{ M}^{-1} \text{ cm}^{-1}$ (OTA^+ , Fig. 3) hence only approximately half of all photons are absorbed by the photosensitizer, the other half directly excites OTA^+ . There is a good spectral overlap between $\text{Ru}(\text{bpy})_3^{2+}$ emission and OTA^+ absorption (Fig. 3) hence one of the key conditions for intramolecular energy transfer is fulfilled. On the other hand, this process is formally spin-forbidden because $\text{Ru}(\text{bpy})_3^{2+}$ is excited to a $^3\text{MLCT}$ state whereas OTA^+ has doublet spin multiplicity in its electronic ground state,³³ and consequently intramolecular energy transfer from photoexcited $\text{Ru}(\text{bpy})_3^{2+}$ to OTA^+ could in principle be relatively inefficient.³⁴ However, our investigations show that CH_3CN solutions of **Ru-OTA**⁺ and **AQ-Ru-OTA**⁺ (prepared by chemical oxidation using $\text{Cu}(\text{ClO}_4)_2$) are essentially non-luminescent. We conclude that energy transfer (EnT in Scheme 3a and b) from photoexcited $\text{Ru}(\text{bpy})_3^{2+}$ to OTA^+ is a rather efficient process, at least when compared to radiative $^3\text{MLCT}$ relaxation. (As noted above, the concentrations of unreacted $\text{Cu}(\text{II})$ under the conditions used for these experiments are marginal hence oxidative bimolecular $^3\text{MLCT}$ quenching by $\text{Cu}(\text{II})$ is unlikely). Thus, ultimately the absorption of a second 450 nm photon leads to excitation of OTA^+ , either directly or indirectly via energy transfer from $\text{Ru}(\text{bpy})_3^{2+}$ (see “either/or” labels in Scheme 3a and b). It is not possible to probe the relevant OTA^+ excited state directly, and its lifetime is unlikely to be much longer than 1 ns. This severely limits the probability for collisional encounters with O_2 and contributes to the relatively low efficiency of the overall charge accumulation process (see below).

Nevertheless, photoexcitation of triarylamine radical cations has been previously reported to trigger oxidation to their dicationic forms,^{33a} and therefore it seems plausible that formation of the second equivalent of $\text{Sc}^{3+}/\text{O}_2^-$ adducts involves directly the excited OTA^+ species. In some cases, phototriggered oxidation of triarylamine cations has been observed to result in carbazole formation,^{33a} but in our compounds this seems unlikely because the addition of triethylamine to the final solutions rapidly leads to the recovery of the **Ru-OTA** and **AQ-Ru-OTA** starting materials.

In the case of the triad, photoexcited OTA^+ can induce intramolecular electron transfer to result in **AQ-Ru-OTA**²⁺, which can be stabilized by Sc^{3+} before reaction with O_2 occurs (bottom line in Scheme 3b). This reaction pathway could contribute to the substantially higher efficiency for charge accumulation in the triad compared to the dyad (see below).

Irrespective of whether the $\text{Ru}(\text{bpy})_3^{2+}$ or the OTA^+ unit of **Ru-OTA**⁺ and **AQ-Ru-OTA**⁺ is excited, reverse electron transfer (from the ruthenium photosensitizer to the oxidized amine) is a viable reaction pathway, which can severely limit the overall quantum yield of the charge accumulation process.

We did also consider the possibility of (thermal) disproportionation of 2 equivalents of OTA^+ to 1 equivalent of OTA^{2+} and 1 equivalent of neutral OTA. This reaction is thermodynamically unfavorable based on the redox potentials from Table 1, and when solutions containing **Ru-OTA**⁺ and **AQ-Ru-OTA**⁺ are left standing in the dark for 60 minutes, no significant formation of OTA^{2+} can be observed in both cases (see ESI,[†] Fig. S1).



Temporal evolution and quantum yield of photoinduced charge accumulation

UV-Vis difference spectra such as those in Fig. 6a and e have been recorded after photo-irradiation over 10–12 well-defined time intervals for the **Ru-OTA** dyad and the **AQ-Ru-OTA** triad. The respective spectra are included in the ESI† (Fig. S2 and S3). Each of these spectra can be adequately fitted by a linear combination of the UV-Vis difference spectra obtained for **Ru-OTA**⁺/**AQ-Ru-OTA**⁺ (green traces in Fig. 3a and b) and for **Ru-OTA**²⁺/**AQ-Ru-OTA**²⁺ (red traces in Fig. 3a and b). Thus, the relative proportions of **OTA**⁺ and **OTA**²⁺ can be quantified at any point in time, and one obtains the data in Fig. 7 (see ESI,† for further details). The irradiation experiments were performed with 3 ml of CH_3CN solutions containing $(1.0 \pm 0.1) \times 10^{-5}$ M **Ru-OTA** or **AQ-Ru-OTA** and 0.02 M Sc^{3+} , using a flux of $(6.74 \pm 0.21) \times 10^{15}$ photons per second at a wavelength of 450 nm.

The circles in Fig. 7a indicate the concentration of **Ru-OTA**⁺ as a function of irradiation time (t). At $t = 0$, there are already (5.6 ± 0.6) μM of **Ru-OTA**⁺ present, and this turned out to be unavoidable in the course of sample preparation. Photo-irradiation leads to a relatively rapid increase of the **Ru-OTA**⁺ concentration up to (9.1 ± 0.9) μM , but then it decreases at the expense of an increase of the **Ru-OTA**²⁺ concentration (squares in Fig. 7a). After an irradiation time of 240 minutes, there is practically no **Ru-OTA**⁺ left, and the sample contains almost exclusively **Ru-OTA**²⁺.

Between $t = 15$ min and $t = 30$ min the increase in **Ru-OTA**²⁺ concentration is approximately linear, and during this period (1.5 ± 0.2) μM of charge-accumulated product have been formed. In the 3 ml volume used for these experiments, this corresponds to $(4.5 \pm 0.6) \times 10^{-9}$ mol of **Ru-OTA**²⁺. In the time period of 15 minutes, $(6.07 \pm 0.19) \times 10^{18}$ photons have reached the sample, corresponding to $(1.01 \pm 0.03) \times 10^{-5}$ mol of photons. Consequently, the quantum yield (ϕ) for the formation of **Ru-OTA**²⁺ is $(4.5 \pm 0.7) \times 10^{-4}$.

Analysis of the UV-Vis difference spectra obtained for the **AQ-Ru-OTA** triad as a function of irradiation time yields the data shown in Fig. 7b (see ESI,† for details). In this case essentially

no unreacted starting material is left at the beginning of the irradiation experiment, and (8.0 ± 0.8) μM of **AQ-Ru-OTA**⁺ and (1.6 ± 0.2) μM of **AQ-Ru-OTA**²⁺ are already present at $t = 0$ (due to unavoidable exposure to light during sample preparation).

In this case, the increase of the **AQ-Ru-OTA**²⁺ concentration is approximately linear between $t = 1$ min and $t = 3$ min. (1.6 ± 0.2) μM of charge-accumulated product are formed during this period, corresponding to $(4.8 \pm 0.6) \times 10^{-9}$ mol in the 3 ml solution.

Given the photon flux reported above, $(1.34 \pm 0.04) \times 10^{-6}$ mol of photons have reached the sample in the 120 s irradiation period. This leads to a quantum yield (ϕ) of $(3.6 \pm 0.6) \times 10^{-3}$ for the formation of **AQ-Ru-OTA**²⁺.

Thus we find that the quantum yield for charge accumulation is a factor of 8 higher for the triad compared to the dyad. We attribute this to the fact that the radical anionic form of the anthraquinone (**AQ**[−]) can be stabilized by Sc^{3+} , making both the **AQ**[−]-**Ru-OTA**⁺ and the **AQ**[−]-**Ru-OTA**²⁺ intermediates more long-lived (in the forms of $\text{Sc}^{3+}/\text{AQ}^{\cdot-}$ -**Ru-OTA**⁺ and $\text{Sc}^{3+}/\text{AQ}^{\cdot-}$ -**Ru-OTA**²⁺, respectively; Scheme 3b). Consequently, the probability for collisional encounters with O_2 is increased, and this has the observed positive effect on the charge accumulation quantum yield.

In a previously investigated antimony porphyrin compound, light-driven conversion of $\text{Sb}(\text{v})$ into $\text{Sb}(\text{iii})$ occurred with a quantum yield of 4×10^{-3} .³⁵

3. Summary and conclusions

Our study demonstrates for the first time that the photodriven accumulation of positive charges on a molecular unit is possible by exploiting metal ion-coupled electron transfer (MCET). Rapid ($>10^{10}$ s^{-1}) photoinduced charge-separation within the dyad and the triad produces the **Ru**⁺-**OTA**⁺ and **AQ**[−]-**Ru-OTA**⁺ states with lifetimes of ≤ 10 ns and 2.4 μs , respectively, and subsequent bimolecular electron transfer with O_2 is facilitated by strong Lewis acid/Lewis base interaction between Sc^{3+} and superoxide anions.^{16,36} The longer lifetime of the charge-separated state in the triad and its stabilization by interaction of the anthraquinone radical anion with Sc^{3+} contribute to the 8 times higher quantum yield for charge accumulation in the triad with respect to the dyad. Absorption of a second 450 nm photon by the same compound leads to the excitation of **OTA**⁺, either directly or *via* intramolecular energy transfer from the $\text{Ru}(\text{bpy})_3^{2+}$ chromophore. The resulting excited species cannot be probed directly but is expected to be short-lived (~ 1 ns), and this significantly limits the efficiency of the overall charge accumulation process. Consequently, light-induced oxidation of **OTA** to its monocationic form is facile, but formation of the dicationic **OTA**²⁺ is comparatively inefficient.

We note that Sc^{3+} and superoxide anions are in a binding equilibrium. A recent study has demonstrated that Sc^{3+} can be liberated from this equilibrium through the addition of protons, and this can lead to the formation of H_2O_2 in the presence of oxygen.³⁷ Hydrogen peroxide may be regarded as a solar fuel.

Our study has provided direct insight into how a combination of intramolecular photoinduced electron transfer reactions and

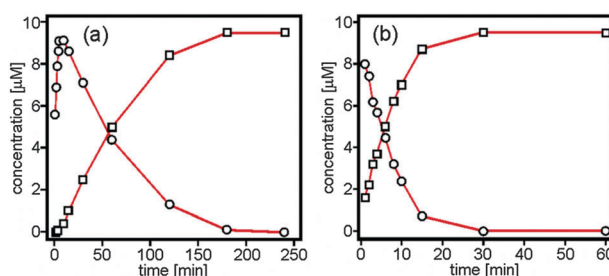


Fig. 7 Concentrations of one-electron and two-electron oxidation products resulting from the photoirradiation of 10^{-5} M solutions of (a) **Ru-OTA** and (b) **AQ-Ru-OTA** in aerated CH_3CN (3 ml volumes). Photoirradiation at 450 nm occurred with a flux of $(6.74 \pm 0.21) \times 10^{15}$ photons per second in the presence of 0.02 M $\text{Sc}(\text{OTf})_3$. The circles correspond to **Ru-OTA**⁺/**AQ-Ru-OTA**⁺ and the squares correspond to **Ru-OTA**²⁺/**AQ-Ru-OTA**²⁺. The individual data points were extracted from the data sets shown in Fig. S2–S4 of the ESI,† The solid red lines are a guide to the eye.



MCET processes can be exploited to achieve the accumulation of two positive charges on a single molecular unit. The findings reported here are relevant in the greater context of artificial photosynthesis.

Acknowledgements

This work was supported by the Swiss National Science Foundation through grant no. 200021_146231/1. Support from COST action CM1202 is acknowledged.

Notes and references

- (a) R. E. Blankenship, *Molecular Mechanisms of Photosynthesis*, Wiley-Blackwell, 2nd edn, 2014; (b) I. Bertini, H. B. Gray, E. I. Stiefel and J. S. Valentine, *Biological Inorganic Chemistry*, University Science Books, Sausalito, California, 2007.
- G. Renger and T. Renger, *Photosynth. Res.*, 2008, **98**, 53.
- (a) X. Sala, S. Maji, R. Bofill, J. Garcia-Anton, L. Escriche and A. Llobet, *Acc. Chem. Res.*, 2014, **47**, 504; (b) S. Neudeck, S. Maji, I. Lopez, S. Meyer, F. Meyer and A. Llobet, *J. Am. Chem. Soc.*, 2014, **136**, 24; (c) R. Lalrempuia, N. D. McDaniel, H. Müller-Bunz, S. Bernhard and M. Albrecht, *Angew. Chem., Int. Ed.*, 2010, **49**, 9765; (d) R. Zong and R. P. Thummel, *J. Am. Chem. Soc.*, 2005, **127**, 12802; (e) S. M. Barnett, K. I. Goldberg and J. M. Mayer, *Nat. Chem.*, 2012, **4**, 498; (f) J. J. Concepcion, J. W. Jurss, M. K. Brennaman, P. G. Hoertz, A. O. T. Patrocinio, N. Y. M. Iha, J. L. Templeton and T. J. Meyer, *Acc. Chem. Res.*, 2009, **42**, 1954; (g) C. W. Cady, R. H. Crabtree and G. W. Brudvig, *Coord. Chem. Rev.*, 2008, **252**, 444.
- (a) T. J. Meyer, *Acc. Chem. Res.*, 1989, **22**, 163; (b) H. B. Gray and A. W. Maverick, *Science*, 1981, **214**, 1201; (c) A. F. Heyduk and D. G. Nocera, *Science*, 2001, **293**, 1639; (d) E. E. Benson, C. P. Kubiak, A. J. Sathrum and J. M. Smieja, *Chem. Soc. Rev.*, 2009, **38**, 89; (e) J. L. Dempsey, A. J. Esswein, D. R. Manke, J. Rosenthal, J. D. Soper and D. G. Nocera, *Inorg. Chem.*, 2005, **44**, 6879.
- (a) A. Magnusson, M. Anderlund, O. Johansson, P. Lindblad, R. Lomoth, T. Polivka, S. Ott, K. Stensjö, S. Styring, V. Sundström and L. Hammarström, *Acc. Chem. Res.*, 2009, **42**, 1899; (b) A. G. Bonn and O. S. Wenger, *Chimia*, 2015, **69**, 17; (c) L. Hammarström, *Acc. Chem. Res.*, 2015, **48**, 840.
- (a) Y. Pellegrin and F. Odobel, *Coord. Chem. Rev.*, 2011, **255**, 2578; (b) G. F. Manbeck and K. J. Brewer, *Coord. Chem. Rev.*, 2013, **257**, 1660; (c) K. Rangan, S. M. Arachchige, J. R. Brown and K. J. Brewer, *Energy Environ. Sci.*, 2009, **2**, 410; (d) K. L. Wouters, N. R. de Tacconi, R. Konduri, R. O. Lezna and F. M. MacDonnell, *Photosynth. Res.*, 2006, **87**, 41; (e) R. Konduri, H. W. Ye, F. M. MacDonnell, S. Serroni, S. Campagna and K. Rajeshwar, *Angew. Chem., Int. Ed.*, 2002, **41**, 3185; (f) R. Konduri, N. R. de Tacconi, K. Rajeshwar and F. M. MacDonnell, *J. Am. Chem. Soc.*, 2004, **126**, 11621; (g) M. P. O'Neil, M. P. Niemczyk, W. A. Svec, D. Gosztola, G. L. Gaines and M. R. Wasielewski, *Science*, 1992, **257**, 63.
- H. M. Zhu, N. H. Song, W. Rodriguez-Cordoba and T. Q. Lian, *J. Am. Chem. Soc.*, 2012, **134**, 4250.
- (a) S. Karlsson, J. Boixel, Y. Pellegrin, E. Blart, H. C. Becker, F. Odobel and L. Hammarström, *Faraday Discuss.*, 2012, **155**, 233; (b) S. Karlsson, J. Boixel, Y. Pellegrin, E. Blart, H. C. Becker, F. Odobel and L. Hammarström, *J. Am. Chem. Soc.*, 2010, **132**, 17977; (c) K. T. Oppelt, E. Woss, M. Stiftinger, W. Schofberger, W. Buchberger and G. Knör, *Inorg. Chem.*, 2013, **52**, 11910.
- (a) K. E. Knowles, M. D. Peterson, M. R. McPhail and E. A. Weiss, *J. Phys. Chem. C*, 2013, **117**, 10229; (b) K. E. Knowles, M. T. Frederick, D. B. Tice, A. J. Morris-Cohen and E. A. Weiss, *J. Phys. Chem. Lett.*, 2012, **3**, 18.
- (a) W. T. Eckenhoff and R. Eisenberg, *Dalton Trans.*, 2012, **41**, 13004; (b) A. R. Parent, R. H. Crabtree and G. W. Brudvig, *Chem. Soc. Rev.*, 2013, **42**, 2247.
- H. Imahori, M. Hasegawa, S. Taniguchi, M. Aoki, T. Okada and Y. Sakata, *Chem. Lett.*, 1998, 721.
- (a) S. M. Arachchige, J. R. Brown, E. Chang, A. Jain, D. F. Zigler, K. Rangan and K. J. Brewer, *Inorg. Chem.*, 2009, **48**, 1989; (b) M. Elvington and K. J. Brewer, *Inorg. Chem.*, 2006, **45**, 5242; (c) M. Elvington, J. Brown, S. M. Arachchige and K. J. Brewer, *J. Am. Chem. Soc.*, 2007, **129**, 10644; (d) S. M. Molnar, G. Nallas, J. S. Bridgewater and K. J. Brewer, *J. Am. Chem. Soc.*, 1994, **116**, 5206; (e) S. Rau, B. Schafer, D. Gleich, E. Anders, M. Rudolph, M. Friedrich, H. Gorls, W. Henry and J. G. Vos, *Angew. Chem., Int. Ed.*, 2006, **45**, 6215; (f) H. Ozawa, M. A. Haga and K. Sakai, *J. Am. Chem. Soc.*, 2006, **128**, 4926.
- (a) A. Fihri, V. Artero, M. Razavet, C. Baffert, W. Leibl and M. Fontecave, *Angew. Chem., Int. Ed.*, 2008, **47**, 564; (b) P. W. Du, J. Schneider, G. G. Luo, W. W. Brennessel and R. Eisenberg, *Inorg. Chem.*, 2009, **48**, 4952.
- R. H. Holm, P. Kennepohl and E. I. Solomon, *Chem. Rev.*, 1996, **96**, 2239.
- (a) P. Du, J. Schneider, L. Fan, W. Zhao, U. Patel, F. N. Castellano and R. Eisenberg, *J. Am. Chem. Soc.*, 2008, **130**, 5056; (b) P. Lei, M. Hedlund, R. Lomoth, H. Rensmo, O. Johansson and L. Hammarström, *J. Am. Chem. Soc.*, 2008, **130**, 26.
- (a) S. Fukuzumi and K. Ohkubo, *Coord. Chem. Rev.*, 2010, **254**, 372; (b) S. Fukuzumi, K. Ohkubo and Y. Morimoto, *Phys. Chem. Chem. Phys.*, 2012, **14**, 8472; (c) S. Fukuzumi, H. Mori, H. Imahori, T. Suenobu, Y. Araki, O. Ito and K. M. Kadish, *J. Am. Chem. Soc.*, 2001, **123**, 12458; (d) S. Fukuzumi, *Chem. Lett.*, 2008, **37**, 808; (e) T. Kawashima, K. Ohkubo and S. Fukuzumi, *Phys. Chem. Chem. Phys.*, 2011, **13**, 3344.
- E. Y. Tsui, R. Tran, J. Yano and T. Agapie, *Nat. Chem.*, 2013, **5**, 293.
- Y. Q. Fang and G. S. Hanan, *Synlett*, 2003, 852.
- (a) V. Hensel, K. Lutzow, J. Jacob, K. Gessler, W. Saenger and A. D. Schlüter, *Angew. Chem., Int. Ed. Engl.*, 1997, **36**, 2654; (b) V. Hensel and A. D. Schlüter, *Liebigs Ann.*, 1997, 303.
- A. G. Bonn, M. Neuburger and O. S. Wenger, *Inorg. Chem.*, 2014, **53**, 11075.

21 (a) A. G. Bonn and O. S. Wenger, *J. Org. Chem.*, 2015, **80**, 4097; (b) Y. Hirao, A. Ito and K. Tanaka, *J. Phys. Chem. A*, 2007, **111**, 2951.

22 J. Hankache, M. Niemi, H. Lemmetyinen and O. S. Wenger, *Inorg. Chem.*, 2012, **51**, 6333.

23 A. B. P. Lever, *Inorg. Chem.*, 1990, **29**, 1271.

24 (a) K. Sreenath, T. G. Thomas and K. R. Gopidas, *Org. Lett.*, 2011, **13**, 1134; (b) V. V. Pavlishchuk and A. W. Addison, *Inorg. Chim. Acta*, 2000, **298**, 97.

25 (a) B. V. Bergeron and G. J. Meyer, *J. Phys. Chem. B*, 2003, **107**, 245; (b) G. A. Heath, L. J. Yellowlees and P. S. Braterman, *J. Chem. Soc., Chem. Commun.*, 1981, 287.

26 (a) J. Hankache and O. S. Wenger, *Chem. – Eur. J.*, 2012, **18**, 6443; (b) F. D. Lewis, A. K. Thazhathveetil, T. A. Zeidan, J. Vura-Weis and M. R. Wasielewski, *J. Am. Chem. Soc.*, 2010, **132**, 444; (c) K. A. Opperman, S. L. Mecklenburg and T. J. Meyer, *Inorg. Chem.*, 1994, **33**, 5295.

27 J. Hankache, M. Niemi, H. Lemmetyinen and O. S. Wenger, *J. Phys. Chem. A*, 2012, **116**, 8159.

28 (a) B. Geiss and C. Lambert, *Chem. Commun.*, 2009, 1670; (b) R. Lopez, A. M. Leiva, F. Zuloaga, B. Loeb, E. Norambuena, K. M. Omberg, J. R. Schoonover, D. Striplin, M. Devenney and T. J. Meyer, *Inorg. Chem.*, 1999, **38**, 2924; (c) G. Steinberg-Yfrach, P. A. Liddell, S. C. Hung, A. L. Moore, D. Gust and T. A. Moore, *Nature*, 1997, **385**, 239; (d) S. L. Larson, C. M. Elliott and D. F. Kelley, *J. Phys. Chem.*, 1995, **99**, 6530.

29 (a) C. G. Hatchard and C. A. Parker, *Proc. R. Soc. A*, 1956, 235, 518; (b) I. P. Pozdnyakov, O. V. Kel, V. F. Plyusnin, V. P. Grivin and N. M. Bazhin, *J. Phys. Chem. A*, 2008, **112**, 8316; (c) E. W. Vitz, *J. Chem. Educ.*, 1981, **58**, 655.

30 R. Nissim, C. Batchelor-McAuley, Q. Li and R. G. Compton, *J. Electroanal. Chem.*, 2012, **681**, 44.

31 J. M. Achord and C. L. Hussey, *Anal. Chem.*, 1980, **52**, 601.

32 M. Montalti, A. Credi, L. Prodi and M. T. Gandolfi, *Handbook of Photochemistry*, CRC Taylor & Francis, Boca Raton, Florida, 2006.

33 (a) D. T. Breslin and M. A. Fox, *J. Org. Chem.*, 1994, **59**, 7557; (b) E. Haselbach and T. Bally, *Pure Appl. Chem.*, 1984, **56**, 1203; (c) P. Carsky and R. Zahradník, *Acc. Chem. Res.*, 1976, **9**, 407.

34 D. Guo, T. E. Knight and J. K. McCusker, *Science*, 2011, **334**, 1684.

35 G. Knör, A. Vogler, S. Roffia, F. Paolucci and V. Balzani, *Chem. Commun.*, 1996, 1643.

36 S. Fukuzumi, K. Okamoto, Y. Yoshida, H. Imahori, Y. Araki and O. Ito, *J. Am. Chem. Soc.*, 2003, **125**, 1007.

37 (a) S. Kato, J. U. Jung, T. Suenobu and S. Fukuzumi, *Energy Environ. Sci.*, 2013, **6**, 3756; (b) Y. Yamada, M. Yoneda and S. Fukuzumi, *Energy Environ. Sci.*, 2015, **8**, 1698.

